© 2019. Published by The Company of Biologists Ltd | Development (2019) 146, dev174300. doi:10.1242/dev.174300

RESEARCH ARTICLE

# A branching gene regulatory network dictating different aspects of a neuronal cell identity

**Johannes Stratmann[1,*], Helen Ekman[1] and Stefan Thor[1,2,‡]**


## ABSTRACT

The nervous system displays a daunting cellular diversity. Neuronal subtypes differ from each other in several aspects, including their neurotransmitter expression and axon projection. These aspects can converge, but can also diverge, such that neurons expressing the same neurotransmitter may project axons to different targets. It is not well understood how regulatory programs converge/diverge to associate/dissociate different cell fate features. Studies of the *Drosophila* Tv1 neurons have identified a regulatory cascade, *ladybird early→collier→apterous/eyes absent→dimmed*, that specifies Tv1 neurotransmitter expression. Here, we conduct genetic and transcriptome analysis to address how other aspects of Tv1 cell fate are governed. We find that an initiator terminal selector gene triggers a feedforward loop that branches into different subroutines, each of which establishes different features of this one unique neuronal cell fate.


**KEY WORDS: Cell fate specification, Terminal selector, Axon pathfinding, Genetic cascades, Feedforward loops**

## INTRODUCTION

The nervous system contains many different neuronal subtypes and understanding cell fate specification remains a major challenge. Mature neurons differ from each other with respect to a number of different properties, including neurotransmitter identity, electrophysiological properties and axon/dendrite morphology. These different properties are not always linked. For example, neurons producing the same neurotransmitter may project axons to different targets, and neurons projecting to the same target may produce different neurotransmitters. In addition, related neurons may originate from different progenitors and different locations with the CNS. This begs the question of how the developmental regulatory machinery can determine which features to combine in order to establish a particular cell fate. Although a number of studies have focused on the genetic programs determining one specific aspect of a neuronal cell fate, few studies have addressed multiple aspects simultaneously. The exception is studies in *C. elegans*, which have involved a comprehensive analysis of the regulatory programs dictating most, if not all, aspects of terminal neuron cell fate for several specific neurons (reviewed by Hobert, 2016; Hobert et al., 2010). This has unravelled several intriguing principles underlying neuronal subtype specification. However, it remains unclear how regulatory cascades are integrated to determine all aspects of neuronal subtype identity in animals with thousands of neurons and hundreds of cell fates.

The Apterous (Ap) neurons of the *Drosophila* ventral nerve cord (VNC) constitute a powerful model for addressing these issues, because of the availability of selective markers and genetic tools, as well as the insight available into their specification that stems from previous extensive work (reviewed by Allan and Thor, 2015). Ap neurons constitute a small subgroup of interneurons that express the Apterous (Ap) LIM-homeodomain factor and the Eyes absent (Eya) transcriptional co-factor and nuclear phosphatase (Fig. 1A) (Lundgren et al., 1995; Miguel-Aliaga et al., 2004). A subset of Ap neurons expresses the Nplp1 neuropeptide: the lateral thoracic Tv1 neurons, part of the thoracic Ap cluster of four cells, and the dorsal medial row of dAp neurons (Fig. 1A,B) (Baumgardt et al., 2007; Park et al., 2004). In line with the different position of the Tv1 and dAp neurons, previous studies have revealed that they originate from two different progenitors (neuroblasts, NBs): NB5-6T and NB4-3, respectively (Baumgardt et al., 2009; Gabilondo et al., 2016). In addition to their expression of the same neuropeptide, Tv1 and dAp neurons also project their axons along a common route, ipsilaterally and anteriorly along the medial-most Fasciclin II (FasII)-positive axon bundle (Fig. 1A,B) (Lundgren et al., 1995). In addition to expressing the Nplp1 neuropeptide, Tv1 and dAp are similar with respect to their secretory properties. Specifically, their neuropeptide expression necessitates the co-expression of a number of genes involved in the processing of neuropeptides, as well as the establishment of secretory large dense-core vesicles (Allan et al., 2005; Park et al., 2004, 2008b). These features are collectively referred to as the regulated secretory pathway (Park and Taghert, 2009). Thus, Tv1 and dAp neurons share three defining features: their axon pathfinding; the expression of the Nplp1 neuropeptide; and the expression of the regulated secretory pathway.

A number of studies have addressed the molecular genetic underpinnings of Tv1 and dAp neuron specification, both with respect to axonal projection, the expression of the Nplp1 neuropeptide and establishment of the regulated secretory pathway. These studies have identified two distinct spatio-temporal combinatorial transcription factor codes, one acting in NB5-6T and the other in NB4-3, that dictate Tv1 and dAp fate, respectively (Gabilondo et al., 2016). In NB5-6T, these upstream cues involve the *ladybird early* (*lbe*) gene, which activates the *collier* gene (*col*; *kn* – Flybase), encoding a COE/EBF transcription factor (Fig. 1B) (Baumgardt et al., 2009; Gabilondo et al., 2016; Karlsson et al., 2010). Lbe and Col then trigger a feed-forward loop (FFL) consisting of Ap, Eya and the Dimmed (Dimm) bHLH transcription factor, which together activate the *Nplp1* gene (Baumgardt et al., 2007; Stratmann and Thor, 2017). In addition, Ap and Eya have been found to play crucial roles in Tv1 and dAp axon pathfinding (Lundgren et al., 1995; Miguel-Aliaga et al.,

[1]Department of Clinical and Experimental Medicine, Linkoping University, SE-581 85 Linkoping, Sweden. [2]School of Biomedical Sciences, University of Queensland, St Lucia QLD 4072, Australia.
*Present address: Max Planck Institute of Molecular Cell Biology and Genetics, 01307 Dresden, Germany.

‡Author for correspondence (stefan.thor@liu.se; s.thor@uq.edu.au)

J.S., 0000-0002-9872-8395; S.T., 0000-0001-5095-541X

**Received 27 November 2018; Accepted 22 February 2019**

Development (2019) 146, dev174300. doi:10.1242/dev.174300

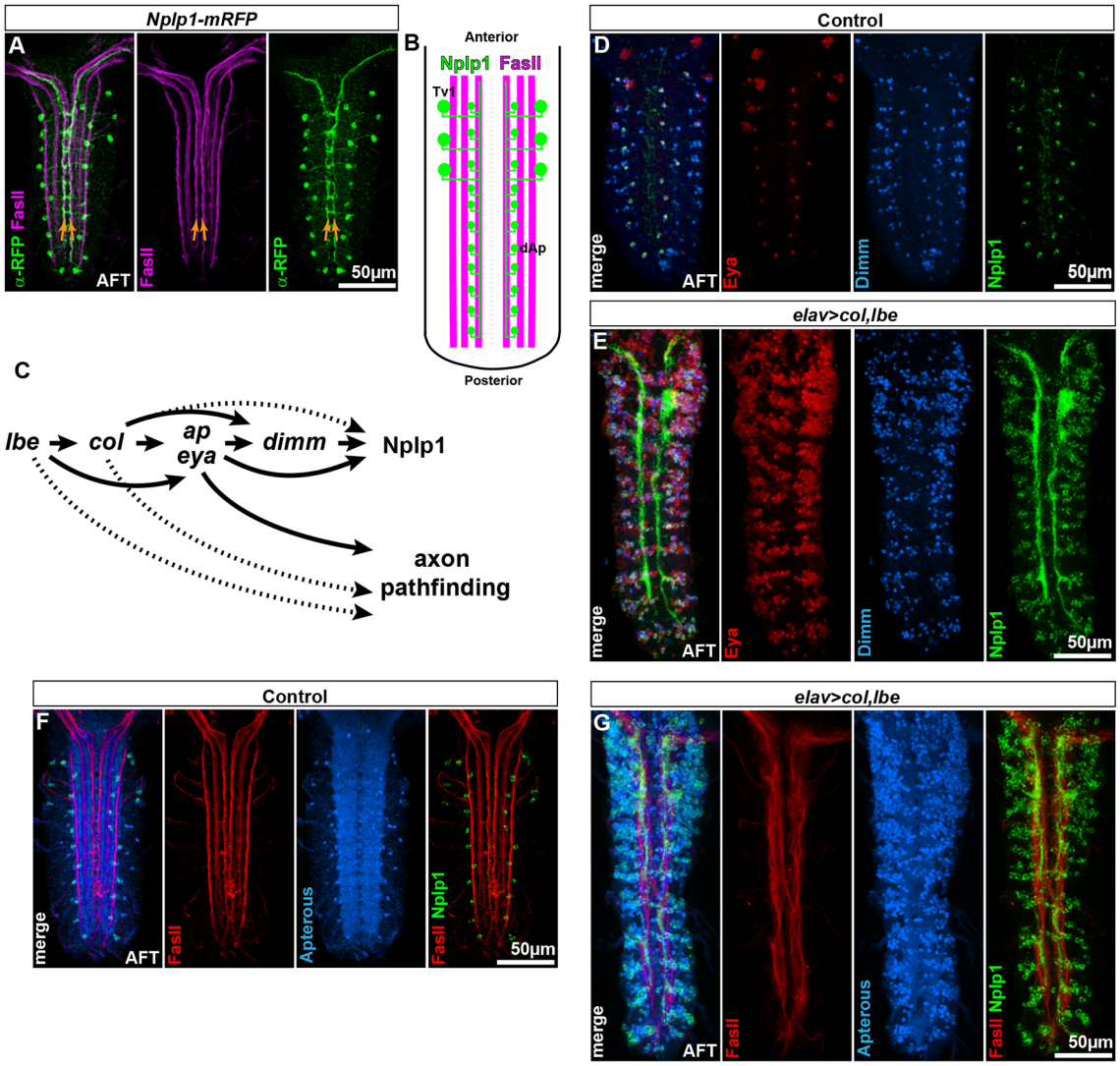


**Fig. 1. Co-misexpression of *col* and *lbe* results in ectopic Tv1 cells.** (A) *Nplp1-CRM-myrRFP* (RFP false coloured in green) and FasII expression at stage AFT reveal the axon projections of the Nplp1-positive neurons. myrRFP and FasII overlap along the medial-most FasII-positive axon bundle (orange arrows). (B) Cartoon depicting that both the Nplp1-positive dorsal dAp neurons, found along the VNC, and the thoracic Tv1 neurons project their axons along the medial FasII-positive bundle. (C) Regulatory cascade for Tv1 specification, with *lbe*, *col*, *ap*, *eya* and *dimm* acting in a feed-forward loop (FFL) to specify the Tv1 cell identity. *ap* and *eya* have previously been shown to be involved in axon guidance. However, the role of *col* and *lbe* in regulating axon projections of the Tv1 neurons, and any downstream genes involved, was hitherto unknown. (D,E) Embryonic stage AFT VNCs stained for Eya, Dimm and Nplp1 in control and *UAS-col,lbe* misexpression, driven by *elav-Gal4*. *col*/*lbe* misexpression (E) results in ectopic Eya, Dimm and Nplp1 expression. (F,G) VNCs of control and *elav-Gal4*/*UAS-col,lbe* misexpression at AFT, stained for FasII, Ap and Nplp1, showing that *col*/*lbe* misexpression (G) results in ectopic Ap and Nplp1 expression. Co-misexpression of *col*/*lbe* also results in changes to the FasII-positive axon scaffold, and accumulation of ectopic Nplp1-positive axons along the medial-most FasII-positive bundle. Genotypes: (A) *Nplp1-CRM-myrRFP*; (D,F) *OregonR*; (E,G) *elav-Gal4*/*UAS-col,UAS-lbe*.

2004), while Dimm appears to be necessary and sufficient for establishing the regulated secretory pathway (Allan et al., 2005; Hamanaka et al., 2010; Hewes et al., 2006; Park et al., 2011, 2004, 2014, 2008a,b). These genetic studies have shed light upon the cell specification of Tv1 and dAp neurons with respect to the neuropeptide Nplp1 and the regulated secretory pathway. However, they have not addressed the role of each regulator with respect to axon pathfinding, or resolved the full gene expression signature of these neurons regarding regulatory cascades and effector outputs.

To address these issues, we focus here on the Tv1 neurons, which are generated by NB5-6T. We find that both *col* and *lbe* are crucial for Tv1 axon pathfinding. In addition, co-misexpression of *col*/*lbe* is sufficient to ectopically re-route other neurons into the Tv1 fascicle. The strength of this effect prompted us to conduct transcriptome analysis, attempting to unravel the full Tv1 signature. As anticipated, this identified *ap*, *eya* and *dimm* as being transcriptionally upregulated. We also observed transcriptional upregulation of many genes involved in the regulated secretory pathway, presumably as an effect of *dimm* upregulation. In addition to *ap*, *eya* and *dimm*, we observed altered expression of two additional transcription factor genes: *nerfin-1* and *Dbx*, as well as of a number of axon pathfinding genes, including *uncoordinated-104* (*unc-104*), *golden goal* (*gogo*) and *futsch*. Mutant and misexpression analysis of the genes identified by transcriptomic analysis revealed different effects upon Tv1 neuron specification. In line with genetic analysis (herein and previously conducted), co-misexpression of *ap*/*eya* followed by transcriptome analysis

Development (2019) 146, dev174300. doi:10.1242/dev.174300

revealed a smaller number of genes that were mis-regulated. Together with previous studies on Tv1 neurons, these findings point to a branching neuronal cell fate specification model, where the different regulators play partly overlapping, but also unique roles with respect to neurotransmitter, axon pathfinding and secretory properties. Such branching regulatory networks are likely to be prevalent in more-complex nervous systems.

## RESULTS

### *ladybird early* and *collier* combinatorially govern Tv1 axon pathfinding and neurotransmitter identity

The activation of the Nplp1 neuropeptide in Tv1 and dAp neurons is controlled by a shared coherent FFL, consisting of *col*, *ap*, *eya* and *dimm* (Baumgardt et al., 2007; Gabilondo et al., 2016). Tv1 and dAp neurons are generated by two different NBs, NB5-6T and NB4-3, respectively, and, hence, the FFL is triggered by two different upstream spatio-temporal combinatorial codes (Baumgardt et al., 2009; Gabilondo et al., 2016; Karlsson et al., 2010). In NB5-6T these upstream cues include the homeobox gene *lbe* (Fig. 1C).

The Tv1 and dAp neurons both project axons ipsilaterally and anteriorly, into a common fascicle that overlaps with the medial-most bundle identified by the axon fascicle marker FasII (Fig. 1A,B) (Lundgren et al., 1995). *ap* and *eya* have both been found to control proper axon pathfinding of Tv1/dAp neurons (Lundgren et al., 1995; Miguel-Aliaga et al., 2004), whereas *dimm* is not involved in axon pathfinding (Allan et al., 2005). The roles of *lbe* and *col* with respect to axon pathfinding have not been addressed previously. To unravel the roles of the identified regulators in axon pathfinding, we focus on the Tv1 neurons.

We have previously found that combinatorial misexpression of *col* and *lbe* was sufficient to trigger widespread specification of ectopic Tv1 neurons, evident by ectopic Ap, Eya, Dimm and Nplp1 expression (Gabilondo et al., 2016). We repeated this experiment, using the pan-neural *elav-Gal4* driver, and confirmed ectopic expression of Ap, Eya, Dimm and Nplp1 (Fig. 1D,E). As anticipated from previous studies (Baumgardt et al., 2009, 2007; Gabilondo et al., 2016; Stratmann et al., 2016), co-misexpression of *col* and *lbe* did not activate expression of the FMRFa neuropeptide, expressed by the Tv4 and SE2 neurons, but rather downregulated its expression (Fig. S1A-H). In addition, based upon the Nplp1 expression, ectopic neurons project axons into a common medial fascicle, similar in location to the normal Tv1/dAp fascicle (Fig. 1D,E). This axon projection effect was also evident when staining for FasII, revealing axon re-routing into the medial-most FasII-positive bundle, and a reduction of the number of FasII-positive bundles (Fig. 1F,G, Fig. S2E-K).

Although both *ap* and *eya* are necessary for Nplp1 expression and proper axon pathfinding of Nplp1-positive neurons, combinatorial misexpression of *ap*/*eya* was not sufficient to trigger ectopic Nplp1 expression (Fig. S2A,B) (Baumgardt et al., 2007). In addition, we did not observe any apparent changes to the FasII-positive axon scaffold (Fig. S2C,D). The striking difference in axon pathfinding effects when comparing *col*/*lbe* co-misexpression with *ap*/*eya* co-misexpression indicates that *col* and *lbe* have roles in axon pathfinding independent of their activation of *ap* and *eya*.

### *ladybird early* and *collier* combinatorially re-route axons to the Tv1 axon fascicle

The disorganized FasII-positive axon scaffold observed in *col*/*lbe* co-misexpression from the pan-neural *elav-Gal4* driver raised the possibility that *col*/*lbe* may be chiefly activating Nplp1 in neurons already projecting in a medial pathway, rather than simultaneously triggering Nplp1 expression and axon projection changes. To address this, we misexpressed *col*/*lbe* using the more-restricted *wg-Gal4* driver, which expresses in only one of the seven rows of NBs: row 5 (Chu-LaGraff and Doe, 1993). To reveal axonal projections, we co-expressed the membrane-targeted *UAS-EGFP$^F$* transgene (Allan et al., 2003). In line with previous mapping studies of NB lineages in the embryonic VNC (Schmid et al., 1999; Schmidt et al., 1997), in control, neurons generated from row 5 NBs project axons along several different pathways, including several of the longitudinal FasII-positive bundles and motor nerves (Fig. 2A, C). Strikingly, in *wg>col,lbe* co-misexpressing embryos, we observed extensive ectopic projections into the medial-most FasII-positive bundle, as well as an apparent complete loss of motor nerve projections (Fig. 2B,D, Figs S3A-N, S4A-C). This effect was evident already at stage (St) 16 but became more pronounced by air-filled trachea (AFT) stage (Fig. 2A-D, Fig. S3A-N).

To determine the individual effects of *col* and *lbe*, we misexpressed them alone and in combination, and quantified the extent of axon re-routing by comparing the integrated GFP-intensity in the medial-most FasII-positive bundle in the region between the commissures (Fig. S5K). We found that *col* single misexpression had a small but significant effect (Fig. S5A,B,E). In contrast, single *lbe* misexpression resulted in a significant reduction of axons in the medial-most FasII-positive bundle (Fig. S5C,E). The reduction of the medial projection in *lbe* single misexpression may be due to the effect of *lbe* acting without *col*. Specifically, early-born NB5-6T neurons, which express *lbe* and not *col* (Baumgardt et al., 2009, 2007; Gabilondo et al., 2016), project to the lateral-most FasII-positive bundle, whereas late-born neurons (Ap neurons), which express *col* and *lbe*, project to the medial-most bundle (Fig. 3A-E). *col*/*lbe* co-misexpression resulted in striking combinatorial effects, with more than a fourfold increase in GFP signal in the medial-most FasII-positive bundle, when compared with control (Fig. S5D,E).

In spite of the lack of obvious effects upon the FasII-positive scaffold in response to *ap*/*eya* co-misexpression, when driven from *elav-Gal4*, the higher resolution of the *wg-Gal4, UAS-EGFP$^F$* driver set-up prompted us to re-address the effects of *ap* and *eya*. Indeed, using this driver-marker combination, we observed weak, but significant, re-routing to the medial-most FasII-positive bundle in both *ap* and *eya* single misexpression (Fig. S5F-H,J). These effects were enhanced in the *ap*/*eya* co-misexpression embryos (Fig. S5I,J). However, the *ap*/*eya* combinatorial effect was weaker than that of *col*/*lbe* co-misexpression, again supporting the notion that *col* and *lbe* have axon pathfinding roles outside of their activation of *ap* and *eya*.

### *collier* and *ladybird early* are necessary for Tv1 axon pathfinding

Next, we addressed the mutant effects of *col* and *lbe* upon Ap neurons and Tv1 axon pathfinding. To achieve this, we could not use *ap*, *eya*, *dimm* or *Nplp1* axonal reporters, because these genes are all downregulated in *col* and *lbe* mutants (Baumgardt et al., 2007; Gabilondo et al., 2016). Hence, we made use of the *lbe(K)-EGFP* transgenic reporter, which labels the entire NB5-6T lineage (Baumgardt et al., 2009). However, because *lbe(K)-GFP* labels the entire lineage, we first needed to map the subset of NB5-6T projections that correspond to the Ap neurons (including Tv1). Hence, we combined *lbe(K)-GFP* with *ap-tau-lacZ* (Lundgren et al., 1995), and co-stained for GFP, β-gal and FasII. This analysis revealed the development of the entire NB5-6T lineage projections, the Ap neuron projections and their relation to the FasII-positive

Development (2019) 146, dev174300. doi:10.1242/dev.174300

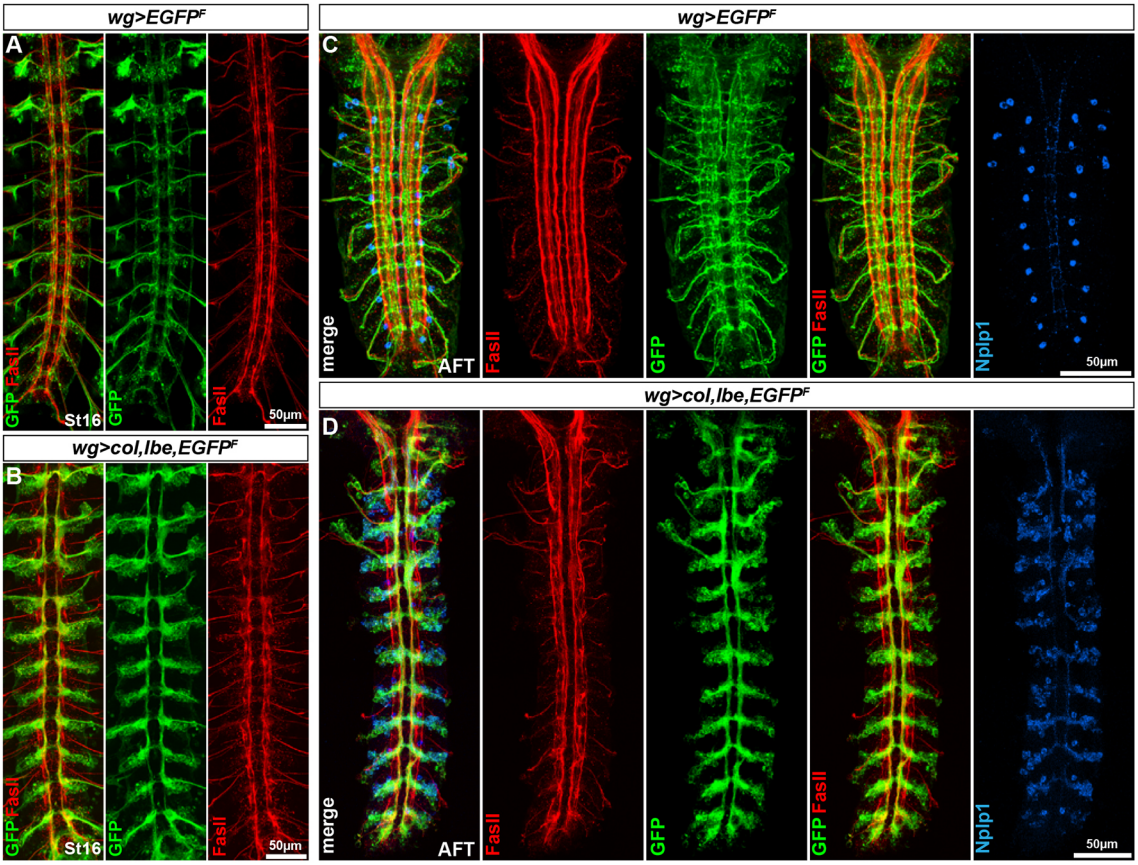


**Fig. 2. *col* and *lbe* are sufficient for axon projection along the medial FasII-positive bundle.** (A-D) Control (A,C) and *UAS-col,lbe* co-misexpression (B,D), driven by the row 5 NB driver *wg-Gal4,UAS-EGFP$^F$* (farnesylated GFP, targeted to cell membranes), stained for GFP, FasII and Nplp1 (in C,D). (A,C) In control, at St16 and AFT, neurons generated by row 5 NBs project axons along different pathways, including several of the longitudinal FasII-positive bundles, as well as the motor nerves. (B,D) In *col*/*lbe* co-misexpression, axons ectopically project primarily along the medial-most FasII-positive bundle, and there is an apparent loss of motor nerve projections. (C,D) *col*/*lbe* co-misexpression driven by *wg-Gal4* also triggers ectopic Nplp1 expression, albeit to a lesser degree than with *elav-Gal4*. Genotypes: (A,C) *wg-Gal4, UAS-EGFP$^F$*/+; (B,D) *wg-Gal4, UAS-EGFP$^F$*/+; *UAS-col,UAS-lbe*/+.

scaffold (Fig. 3A-E). We found that the earlier-born NB5-6T neurons projected into the lateral-most FasII-positive bundle, as well as across the anterior commissure, whereas Ap axons can be observed at St16 joining the medial-most bundle (Fig. 3A-E). With this information at hand, we introduced the *lbe(K)-GFP* transgene into the *col* and *lbe* mutants, and assayed the effects upon the Ap axons, including Tv1. In both *col* and *lbe* mutants, we observed a failure of the Ap axons to project into the medial-most FasII-positive bundle, apparent both at St16, St17 and stage AFT (Fig. 3F-H, Fig. S6A-E). In line with the finding that early-born NB5-6T neurons, which express *lbe* but not *col*, project laterally or across the anterior commissure (Fig. 3A-E), we observed defects in these projections in *lbe* mutants, whereas *col* only affected the medial-most projections (Fig. 3F,G).

The mutant and misexpression analyses demonstrate that *col* and *lbe* are necessary, and in part sufficient, for Tv1 axon pathfinding. Similarly, *ap* and *eya* are also necessary and, to a lesser extent, sufficient for Tv1 axon pathfinding. This raises the issue of whether or not *lbe* and *col* act only via *ap* and *eya* or whether they have roles outside this function. To address this, we misexpressed *col* in the NB5-6 lineage, using a *lbe(K)-Gal4, UAS-EGFP$^F$* combination, in control as well as in *ap* and *eya* mutants. Because of the effect of single misexpression of *lbe* from *wg-Gal4*, i.e. routing of axons into the lateral-most FasII-positive bundle, we overexpressed *lbe* in *ap* or *eya* mutants. We analysed abdominal segments, because the lack of Ap neurons in the NB5-6A lineages (Karlsson et al., 2010) results in the absence of axons from this lineage in the medial-most FasII-positive bundle (Fig. S7A). In control, similar to the effects of *elav-Gal4* and *wg-Gal4*, misexpression of *col* from *lbe(K)-Gal4* triggers ectopic axon projections into the medial-most FasII-positive bundle (Fig. S7B). Strikingly, in both *ap* and *eya* mutants, *col* is still able to trigger these ectopic axon projections (Fig. S7C-F).

To summarize, *col*, *lbe*, *ap* and *eya* are all crucial for proper axon pathfinding of Ap neurons, including the Tv1 neuron. Although *col*/*lbe* co-misexpression robustly activates Ap and Eya, the weaker effects of *ap*/*eya* co-misexpression and the misexpression effects of *col* in *ap* or *eya* mutant backgrounds indicate that *col* and *lbe* have axon pathfinding roles in addition to their activation of *ap* and *eya*.

### Transcriptome analysis of *col*/*lbe* co-misexpression embryos reveals activation of the Tv1 cell fate cascade

Co-misexpression of *col*/*lbe* results in robust reprogramming of many neurons to Tv1 cell fate, as apparent from ectopic expression of the Tv1 regulatory cascade (Ap, Eya and Dimm), the Nplp1 neurotransmitter and Tv1-like axon pathfinding. These results suggested that *col*/*lbe* co-misexpression followed by transcriptome analysis of embryonic RNA could allow for the identification of the entire Tv1 cell signature, as well as identify novel regulators and effectors involved in Tv1 fate. To this end, we co-misexpressed

Development (2019) 146, dev174300. doi:10.1242/dev.174300

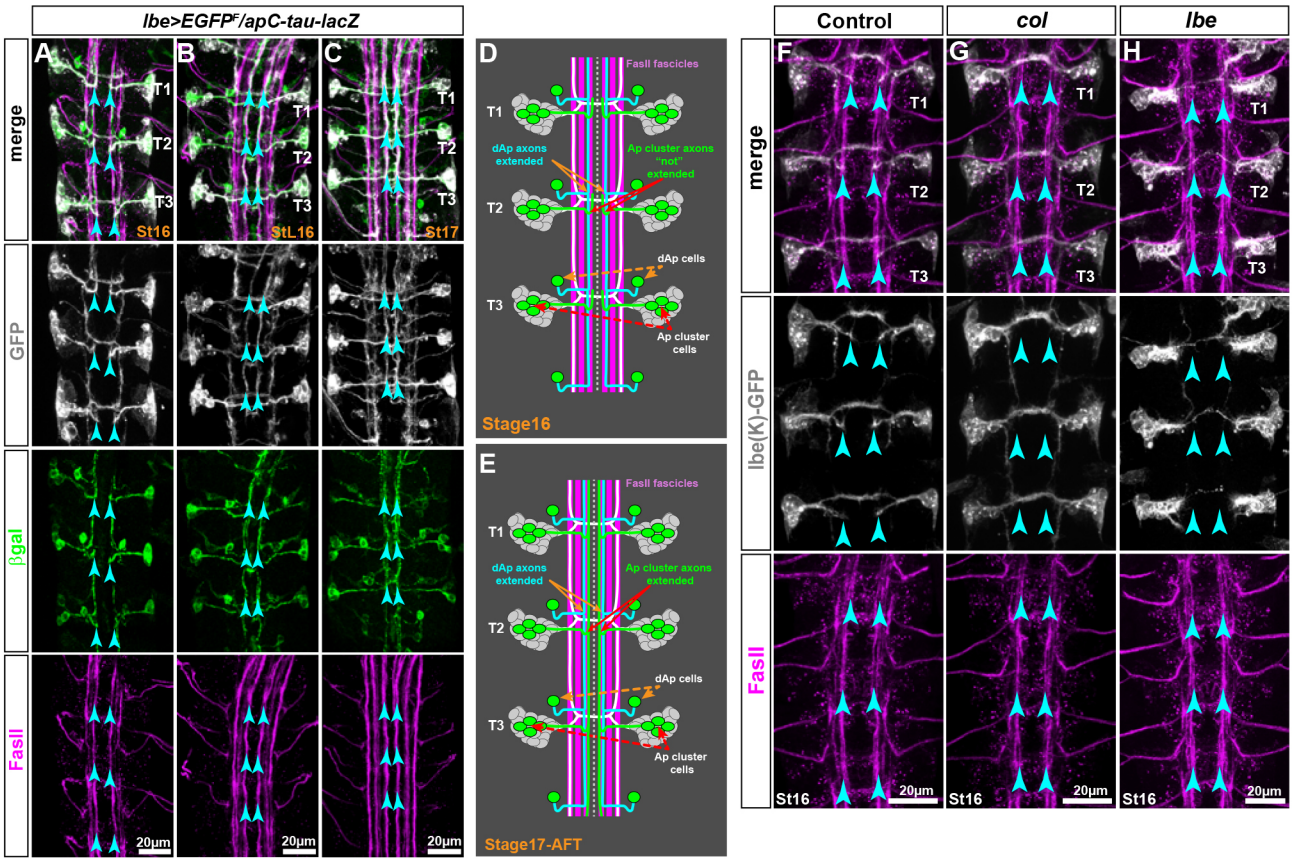


**Fig. 3. *col* and *lbe* are necessary for axon projection along the medial FasII-positive bundle.** (A-E) Axon projections of all NB5-6T neurons at St16-St17, visualized using *lbe(K)-Gal4>UAS-EGFP^F*, and of Ap neurons, visualized using *apC-tau-lacZ*, stained for β-gal, GFP and FasII. Ap axons label a subset of NB5-6T neurons and project into the medial-most FasII-positive bundle (blue arrowheads). (F-H) Axon projections of NB5-6T neurons at St16, visualized using *lbe(K)-Gal4>UAS-EGFP^F*, in control, *col* and *lbe* mutants. In control, the Ap cluster neurons in NB5-6T, including the Tv1 neuron, project into the medial-most FasII-positive bundle. In *col* and *lbe* mutants, these axonal projections towards the medial FasII-positive bundle are absent (blue arrowheads). Genotypes: (A-C) *apC2.1-tau-lacZ/ lbe(K)-Gal4/UAS-EGFP^F*; (F) *lbe(K)-Gal4, UAS-EGFP^F/+*; (G) *col^1/col^3*; *lbe(K)-Gal4/UAS-EGFP^F*; (H) *lbe(K)-Gal4/UAS- EGFP^F; lbe^12C5/lbe^Df*.

*lbe/col* and analysed the transcriptome, using whole-embryo RNA-seq, both at St16 and stage AFT.

As anticipated, we found that the entire known Tv1 regulatory cascade was activated, including *ap*, *eya* and *dimm*, as well as *Nplp1*, both at St16 and stage AFT (Fig. S8A,B). As noted above, owing to the temporal progression of the Ap neuron regulatory cascade (Baumgardt et al., 2009, 2007; Gabilondo et al., 2016; Stratmann et al., 2016), *col*/*lbe* co-misexpression does not trigger ectopic expression of the FMRFa neuropeptide (Fig. S1A-N) (Gabilondo et al., 2016), which is expressed by the Tv4 Ap neurons. In line with these previous findings, we did not observe upregulation of the *FMRFa* gene (Fig. S8A,B).

### *col*/*lbe* co-misexpression activates *dimm* and, therefore, the regulated secretory pathway

Previous studies have demonstrated that *dimm* controls the regulated secretory pathway, being both necessary and sufficient to directly activate a number of genes in this pathway (Allan et al., 2005; Hamanaka et al., 2010; Hewes et al., 2006; Park et al., 2011, 2004, 2014, 2008a,b). Because *col*/*lbe* activates *dimm* expression, we analysed the expression of 21 of the previously identified *dimm* target genes in the regulated secretory pathway. This analysis revealed that *col*/*lbe* co-misexpression significantly activated expression of 14 of these 21 genes, with the remaining six showing a trend upwards, albeit non-significant (Fig. S8C).

### *col*/*lbe* and *ap*/*eya* co-misexpression regulates axon pathfinding genes

Next, we turned to the axon pathfinding aspect of Tv1 cell fate. Because the aforementioned results showed that not only *col*/*lbe* but also *ap*/*eya* are involved in the axon pathfinding of Tv1 neurons (this study; Lundgren et al., 1995; Miguel-Aliaga et al., 2004), we also analysed the transcriptome for combinatorial and single misexpression of all four genes. Focusing first on co-misexpression of *col*/*lbe* versus *ap*/*eya*, at stage AFT, this analysis revealed twofold changes (2FC) in expression of 1075 and 650 genes, respectively (Fig. 4A,B). A smaller number of genes showed altered expression at St16 (Fig. S9A,E). There was considerable overlap in the gene expression profiles, with 458 genes affected by both *col*/*lbe* and *ap*/*eya* (Figs S9E, S10B). Gene ontology (GO) filtering of the overlapping set of genes revealed a diverse set of molecular functions, biological processes and cellular components (Fig. S10A-C).

GO filtering for the 416 *Drosophila* genes identified as 'neuron projection development' revealed that *col*/*lbe* and *ap*/*eya* co-misexpression altered expression of 13 and seven of these genes, respectively (Fig. 4A,B). As anticipated, *col* itself (*knot*; *kn*) was identified in the *col*/*lbe* co-misexpression samples, as well as *ap* and *eya* in the *ap*/*eya* co-misexpression samples (Fig. 4A,B). Surveying the overlap in gene expression between *col*/*lbe* and *ap*/*eya* within the GO category 'neuron projection development', we

Development (2019) 146, dev174300. doi:10.1242/dev.174300

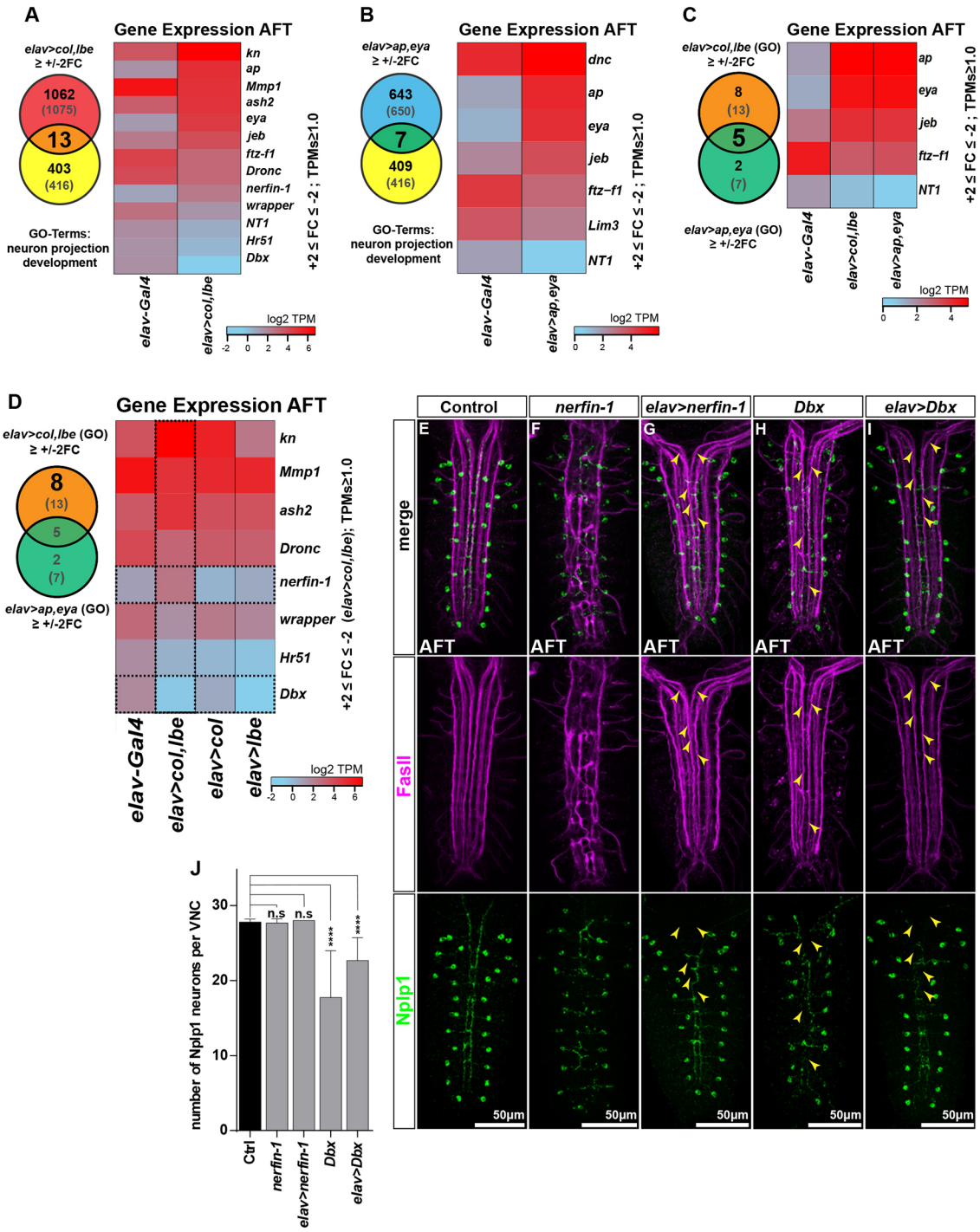


**Fig. 4.** See next page for legend.

identified five genes whose expression was changed twofold in both genotypes, indicating that those factors are regulated by *col*/*lbe* via *ap*/*eya*. In addition to *ap* and *eya* themselves, these were: *jelly belly*, which was up-regulated; and *ftz-f1* and *Neurotrophin 1* (*NT1*), which were downregulated (Fig. 4C).

### The *nerfin-1* and *Dbx* genes control axon pathfinding

Next, we focused on the eight 'neuron projection development' genes regulated by *col*/*lbe* and not by *ap*/*eya*. To address the combinatorial action of *col*/*lbe*, we chose to include the RNA-seq results from the *col* and *lbe* single misexpression in the heatmap, regardless of their fold-change value. We find a strong combinatorial effect in the RNA-seq data of *col*/*lbe* on *nerfin-1* (zinc finger, C2H2-type; vertebrate: NSM1/2), which is upregulated by *lbe/col* co-misexpression, but not in the *col* and *lbe* single misexpression experiments (Fig. 4D). This effect was confirmed by *in situ* hybridization, which revealed an apparent upregulation of *nerfin-1* in the *elav>col,lbe* embryonic VNC (Fig. 5I-J). Previous studies of *nerfin-1* have revealed that its mRNA is expressed by most, if not all, VNC NBs, with Nerfin-1 protein being restricted to a subset of NBs and their daughter cells (Kuzin et al., 2005; Stivers et al., 2000). Both *nerfin-1* mutants and misexpression

Development (2019) 146, dev174300. doi:10.1242/dev.174300

**Fig. 4. Transcriptome analysis identifies *Dbx* and *nerfin-1*.** (A) Venn diagram of 1075 genes (red circle) with a twofold change (2FC) difference in TPMs between control (*elav-Gal4*) and *col*/*lbe* co-misexpression (*elav-Gal4*/*UAS-col,lbe*) at stage AFT. GO-term genes involved in neuron projection and development, containing 416 genes (yellow circle), shows an overlap of 13 genes. Overlapping genes are plotted in a heatmap based on their log2 transformed TPM values. (B) Venn diagram of 650 genes, showing a 2FC difference in TPMs between *UAS-ap,eya* co-misexpression at stage AFT in comparison with the control (*elav-Gal4*). When this is compared with the GO-term gene list for neuron projection and development containing 416 genes, there is an overlap of seven genes. Overlapping genes are plotted in a heatmap based on their log2 transformed TPM values. (C) Venn diagram of the comparison of the 13 genes overlapping between *col*/*lbe* co-misexpression and the GO-gene list (in A) with the seven genes overlapping between *ap*/*eya* co-misexpression and the GO-gene list (in B). Genes overlapping between the two data sets are shown in the heatmap based on their log2 transformed TPM values. (D) Venn diagram of the comparison of the 13 genes overlapping between *col*/*lbe* co-misexpression and the GO-gene list (in A) with the seven genes overlapping between *ap*/*eya* and the GO-gene list (in B). The eight genes altered by *col*/*lbe* co-misexpression are shown in the heatmap based on their log2 transformed TPM values (2FC, vertical black dashed box), including the TPMs of *lbe* and *col* single misexpression. Single misexpression of either *col* or *lbe* has no impact on *nerfin-1* expression, whereas the co-misexpression of *col*/*lbe* shows an upregulation compared with both control and single misexpression experiments (overlap black dashed outlines). *Dbx* is downregulated in both *col* and *lbe* single misexpression compared with the control; however, only *lbe* and *col*/*lbe* misexpression downregulate *Dbx* by 2FC (overlap is indicated by black dashed outlines). (E-I) VNCs stained for FasII and Nplp1 at stage AFT in control, *nerfin-1* and *Dbx* mutants, and in misexpression mutants. (F) In *nerfin-1* mutants, both the FasII-positive axon scaffold and projections of the Nplp1-positive cells are severely disrupted. (G) Misexpression of *UAS-nerfin-1* from *elav-Gal4* results in distorted axonal projections of the Nplp1-positive cells, and axons fail to project ipsilaterally and anteriorly (yellow arrowheads). The FasII-positive axon scaffold, however, is largely intact. (H) *Dbx* mutants show no defects with regards to the FasII-positive axon scaffold. The axon projections of the Nplp1-positive neurons are severely affected and fail to project along the medial FasII-positive fascicle (yellow arrowheads). (I) Misexpression of *UAS-Dbx* from *elav-Gal4* shows axon pathfinding defects with regards to Nplp1-positive axons, while the FasII-positive fascicles are unaffected (yellow arrowheads). (J) Quantification of Nplp1-positive cells shows that neither *nerfin-1* mutants nor *UAS-nerfin-1* misexpression changes the Nplp1-positive cell numbers. Both *Dbx* mutants and *UAS-Dbx* misexpression results in reduced Nplp1-positive cell numbers (****$P \leq 0.0001$, $n=3$ biological replicates, Student's *t*-test; data are mean±s.d.). Genotypes: (A-D) Control, *elav-Gal4*/+, misexpression and *elav-Gal4*/*UAS-cDNA*s; (E) *OregonR*; (F) $nerfin\text{-}1^{DF}/nerfin\text{-}1^{D159}$; (G) *elav-Gal4*/*UAS-nerfin-3xHA*; (H) $Dbx^{D48}/Dbx^{D48}$; (I) *elav-Gal4*/*UAS-Dbx*.

resulted in axon-pathfinding defects in the developing VNC (Kuzin et al., 2005). To test the roles of *nerfin-1* in Tv1 axon pathfinding, we analysed mutants and misexpression at stage AFT, and monitored potential pathfinding by staining for FasII and Nplp1. *nerfin-1* mutants showed strongly disorganized FasII-positive axon bundles and, in addition, disorganized or absent Nplp1-positive axons (Fig. 4E,F). Misexpression of *nerfin-1* from *elav-Gal4* showed a milder phenotype with respect to the FasII-positive bundles, but disorganized Nplp1 axon projections, which fail to project towards the medial-most FasII-positive bundle (Fig. 4G). Strikingly, however, Nplp1 expression was apparently unaffected in *nerfin-1* mutants or misexpression (Fig. 4J). On analysing Nerfin-1 expression, we found that Nerfin-1 is expressed in the NB5-6T lineage and Ap cluster neurons, evident by overlap with *lbe(K)-GFP* and Eya, at St14 and late St15 (StL15). At St16, Nerfin-1 expression is absent from the Ap cluster (Fig. S11A-D). This prompted us to test whether Nerfin-1 can be activated or maintained in the NB5-6T lineage at St16, when *col*/*lbe* are co-misexpressed from the NB5-6 lineage-specific driver *lbe(K)-Gal4*. Indeed, we find that *col*/*lbe* co-misexpression results in a minor, yet significant, increase of Nerfin-1-positive cells in the NB5-6T lineage (Fig. 5A,B,G). Next, we quantified Nerfin-1-positive cells in *col* and *lbe* mutants in the NB5-6T lineage. Based upon the dynamic Nerfin-1 expression, we decided to assess Nerfin-1 cell numbers at an earlier stage than St16, i.e. StL15. However, quantification of Nerfin-1-positive cells in both *col* and *lbe* mutants did not show any significant differences in cell number (Fig. 5C,D,G). We further analysed the expression of Nerfin-1 in *ap* and *eya* mutants, and, in line with the lack of upregulation of nerfin-1 by *elav>ap,eya* in the RNA-seq data, mutant analysis did not reveal any apparent effects on Nerfin-1 expression (Fig. S12A-H).

In contrast to *nerfin-1*, the RNA-seq revealed that *Dbx* (homeobox factor; vertebrate: DBX1/2, BARX1) was downregulated in *lbe/col* co-misexpression, and also strongly affected by a single misexpression of *lbe* (Fig. 4D). Similarly, RNA-seq at St16 revealed a strong combinatorial effect of *lbe/col* on *Dbx* (Fig. S9D). In line with these findings, *col*/*lbe* co-misexpression, from *elav-Gal4*, resulted in significantly decreased numbers of Dbx cells, both in thoracic and abdominal segments (Fig. 6A,B,G). However, *col* or *lbe* mutants did not show significant differences in Dbx-positive cells, in either thoracic or abdominal segments (Fig. 6C-F,H,I). Previous studies revealed that *Dbx* mutants did not show an apparent axon pathfinding phenotype, whereas *Dbx* misexpression led to a decrease in the ability of many neurons to extend axons (Lacin et al., 2009). In agreement with this, we observed apparently intact FasII-positive bundles in *Dbx* mutants. In contrast, there were severe effects on the axon projections of the Nplp1 axons, characterized by a failure to project along the medial-most FasII-positive bundle (Fig. 4H). *Dbx* misexpression, under control of *elav-Gal4*, showed no apparent effect on the FasII-positive bundles, but projection defects of Nplp1 axons along the medial-most FasII-positive bundle (Fig. 4I). Quantification of Nplp1-positive cells in the *Dbx* mutant and misexpression embryos surprisingly revealed a partial loss of Nplp1-positive cells in both cases (Fig. 4J). These findings prompted us to further address the effect of *Dbx* on Tv1 cells, by analysing additional Tv1/Ap cluster markers, at stage AFT. Looking first at Col, Ap, Eya and Nplp1, we noted that whereas Ap clusters were present in each hemi-segment of both *Dbx* and misexpression mutants, there was an apparent mis-specification of the Ap cluster cells, with a frequent loss of Nplp1 expression (Fig. S13A-G). However, we also noted some cases of an extra Nplp1-expressing cell in the Ap cluster (Fig. S13A-G). This notion was confirmed by analysis of Dimm, together with Ap, Eya and Nplp1, which also revealed that both *Dbx* and misexpression mutants displayed a mixed phenotype with either loss of, or extra, Dimm cells in the Ap cluster (Fig. S14A-E). Previous studies on *Dbx* revealed it to be expressed in neurons stemming from five NBs, none of which corresponds to NB5-6 or NB4-3 (Lacin et al., 2009) (the NBs that generate Ap neurons); indeed, we observed no apparent overlap between Dbx and Ap in postmitotic cells (Fig. 6A). To determine whether Dbx is expressed earlier in the NB5-6T lineage, perhaps in the NB itself, we analysed Dbx expression in NB5-6T during St12-St14. However, we did not, detect any apparent expression in the lineage at these stages (Fig. S15A-F).

### Analysis of 1.5FC revealed Tv1 axon pathfinding genes

The scarcity of axon pathfinding genes in the 2FC group in the RNA-seq data prompted us to analyse genes with a fold-change of ≥1.5. Not surprisingly, this expanded the number of genes with significantly altered expression to 3174 for *elav>col/lbe* and 2194 for *elav>ap/eya* (Fig. S16A,B). This also expanded the subset of

Development (2019) 146, dev174300. doi:10.1242/dev.174300

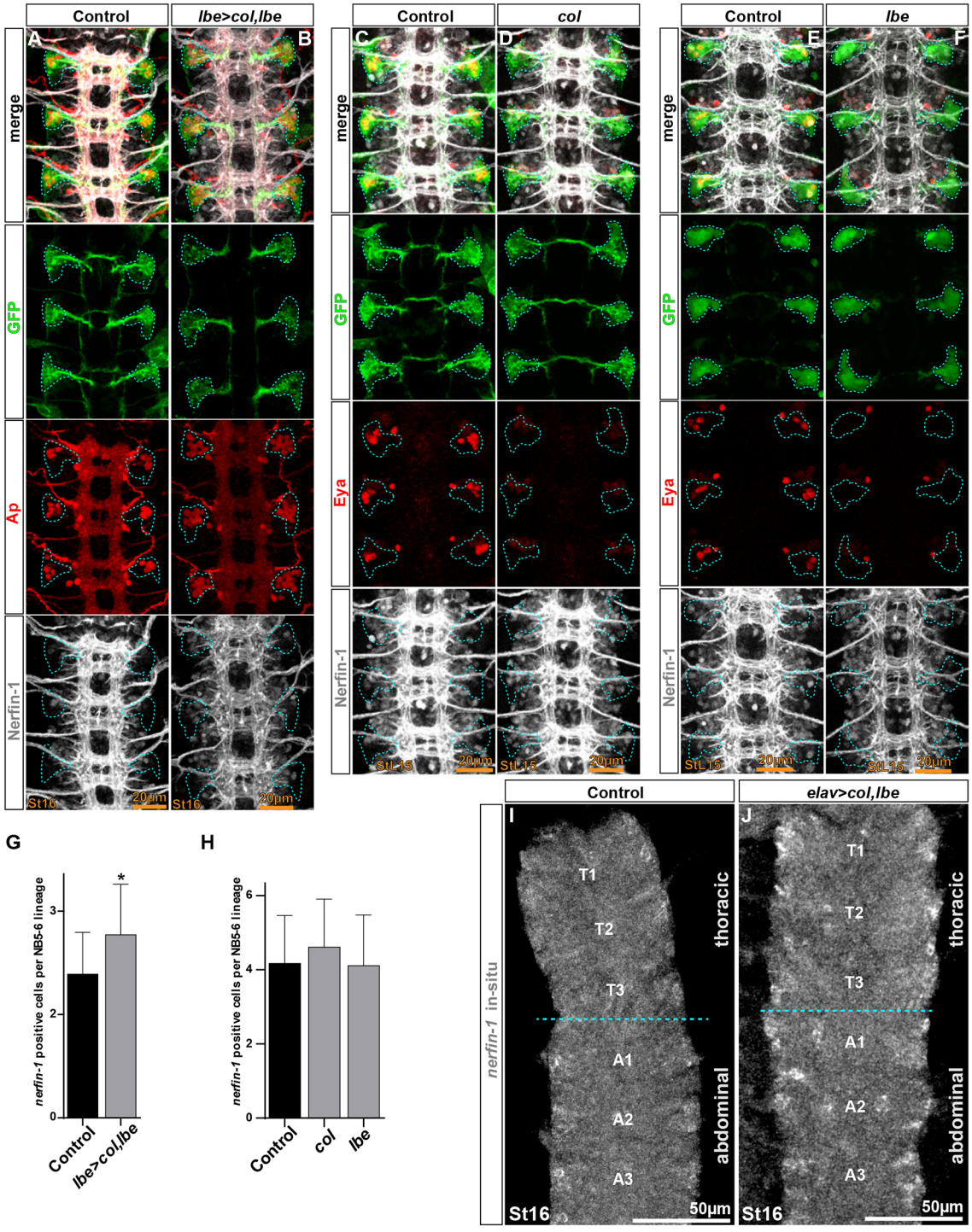


**Fig. 5. Nerfin-1 expression is activated by *col*/*lbe* misexpression, but unaffected in *col* or *lbe* mutants.** (A,B) VNCs stained for GFP, Ap and Nerfin-1 in control and *UAS-col,lbe* co-misexpression in the NB5-6T lineages (cyan dashed lines) under the control of *lbe(K)-Gal4* at St16. *col*/*lbe* co-misexpression triggers an increase in Nerfin-1-expressing cells. (C-F) VNCs stained for GFP, Eya and Nerfin-1 in control (C,E), *col* (D) and *lbe* (F) mutants at StL15. While Eya expression is lost in both *col* and *lbe* mutants, there is no obvious effect on Nerfin-1 expression. Cyan dashed lines indicate the location of the NB5-6T lineage. (G) Quantification of Nerfin-1-positive cells in the NB5-6T lineages (outlined in A,B) shows that the *col*/*lbe* co-misexpression results in significantly more cells than in the control (**P*=0.01, $n \geq 18$ lineages, Student's *t*-test; data are mean±s.d.). (H) Quantification of Nerfin-1-positive cells in the NB5-6T lineage (outlined in C-F) in *col* and *lbe* mutants reveals no significant differences ($n \geq 18$ lineages, Student's *t*-test±s.d.). (I,J) RNA fluorescent *in situ* hybridization for *nerfin-1* in control (I) and *elav>col,lbe* co-misexpression (J) embryos at St16 in thoracic (T1-T3) and abdominal (A1-A3) VNC segments. (J) In *elav>col,lbe* co-misexpression, the *nerfin-1* signal is apparently increased, when compared with control (I). Genotypes: (A,C) *lbe(K)-Gal4,UAS-EGFP$^{F}$*; (B) *lbe(K)-Gal4,UAS-EGFP$^{F}$/UAS-col, UAS-lbe*; (D) *col$^{1}$/col$^{3}$;lbe(K)-Gal4/UAS-EGFP$^{F}$*; (E) *lbe(K)-GFP*; (F) *lbe(K)-GFP/+;lbe$^{12C005}$/lbe$^{Df}$*; (I) *OregonR*; (J) *elav-Gal4/UAS-col,UAS-lbe*.

genes belonging to the 'neuron projection development' GO class: 65 for *col/lbe* and 52 for *ap/eya* (Fig. S16A,B). Comparing these two subsets to each other revealed extensive overlap (Fig. S16C). Given the potent role of *col/lbe* in controlling Tv1-type axon projection, in part independent of *ap/eya*, we focused further upon the 'neuron projection development' genes altered by *col/lbe* but

Development (2019) 146, dev174300. doi:10.1242/dev.174300

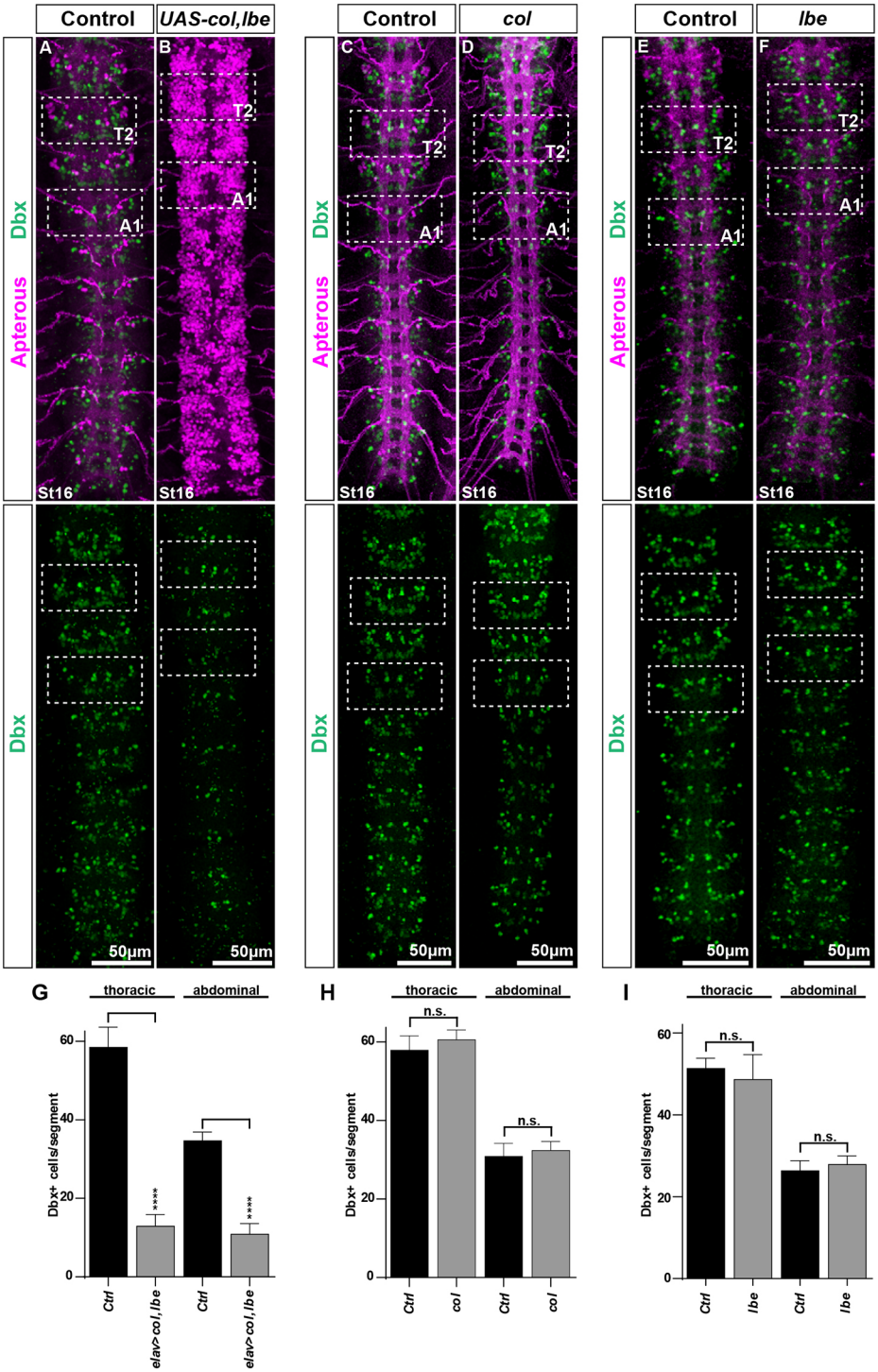


**Fig. 6. *col* and *lbe* repress Dbx expression.** (A-F) Embryonic VNCs stained for Ap and Dbx in control (A,C,E), *col*/*lbe* co-misexpression (B), *col* mutants (D) and *lbe* mutants (F) at St16. (A,B) Misexpression of *col*/*lbe* from *elav-Gal4* results in ectopic Ap neurons and reduction of Dbx-expressing cells. (C,D) *col* mutants show reduction of Ap cells, but no reduction of Dbx-positive cells. (E,F) *lbe* mutants show reduction of Ap cells, but no reduction of Dbx-positive cells. (G-I) Quantification of Dbx-positive cell numbers in thoracic and abdominal segments (example segments are outlined with dashed white boxes in A-F). (G) In *col*/*lbe* co-misexpression, the Dbx-positive cell numbers are significantly reduced compared with control, in both thoracic and abdominal segments (****$P \leq 0.0001$, $n \geq 9$ segments, Student's *t*-test; data are mean±s.d.). (H) In *col* mutants the Dbx-positive cell numbers are not affected ($n=9$ segments, Student's *t*-test; data are mean±s.d.). (I) In *lbe* mutants, the Dbx-positive cell numbers are not affected ($n=9$ segments, Student's *t*-test; data are mean±s.d.). In all cases, Dbx-positive cell numbers are lower in the abdominal segments than in the thoracic segments. Genotypes: (A) *elav-Gal4*/+; (B) *elav-Gal4*/*UAS-col,UAS-lbe*; (C,E) OregonR; (D) $col^{1}/col^{3}$; (F) $lbe^{Df}/lbe^{12C00}$.

not *ap/eya*, and in particular those most effectively regulated by *col/lbe* co-misexpression as opposed to single misexpression. In this group, several of the upregulated genes stood out based upon their previously described roles in 'neuron projection development', including *golden goal* (*gogo*), *uncoordinated-104* (*unc-104*) and *futsch* (Fig. S16D) (Berger et al., 2008; Hummel et al., 2000; Medina et al., 2006; Roos et al., 2000; Tomasi et al., 2008). To address the possible role of these three genes during Tv1 axon pathfinding, we analysed mutants with the Nplp1 and FasII markers. None of the mutants displayed loss of Nplp1 expression in cell bodies (Tv1 or dAp). However, *gogo* and *futsch* mutants both displayed an apparent disorganization of Tv1 axons (Fig. S17A,B,D,E). While *unc-104* mutants displayed Nplp1 expression in cell bodies, there was a complete loss of Nplp1-positive axonal projections (Fig. S17C). The *unc-104* phenotype prompted us to introduce the *Nplp1-CRM-myrRFP* transgene into the *unc-104* background, which revealed that Tv1 axons did indeed project normally in this mutant (Fig. S17F,G). This finding is in line with previous studies, demonstrating that *unc-104*, which encodes a Kinesin-like molecule, is crucial for dense core vesicle axon transport and, hence, neuropeptide transport (Barkus et al., 2008; Lim et al., 2017).

Development (2019) 146, dev174300. doi:10.1242/dev.174300

### Overlap between transcriptome changes and DNA binding

Previous ChIP-seq analysis of Col, from whole mid-embryo chromatin, identified ∼400 genes (de Taffin et al., 2015). We compared this gene list with our RNA-seq lists for *elav>col*, both the 1.5-fold change and 2.0-fold change, at St16 and AFT, and found a number of overlapping genes (Fig. S18A-D). These included *nerfin-1*, *Dbx* and *ap*. In addition, the Col ChIP-seq study also identified *eya* as a direct target of Col (de Taffin et al., 2015). Previous gene-focused studies have also provided support for direct binding of Lbe on *col*, Col on *ap*, *eya* and *dimm*, Ap on *dimm* and *Nplp1*, and Dimm on *Nplp1* (Stratmann and Thor, 2017). In addition, genome-wide analysis of Dimm DNA binding (Hadžić et al., 2015) revealed direct interaction with many of the regulated secretory pathway genes (genes in red in Fig. S8), and, furthermore, the direct regulation of *Phm* has been observed in directed studies (Park et al., 2008a). Hence, a substantial part of the regulatory cascade for Tv1 cell fate apparently involves direct gene regulation.

### Minimal overlap between CNS RNA-seq data and previous muscle RNA-array data for Ladybird early

A previous study addressing Lbe target genes in muscle cells, by using muscle-specific RNAi and muscle-specific misexpression, resulting in the identification of 117 genes with a high fold change (Junion et al., 2007). We compared these results with our CNS-targeted RNA-seq data for *elav>lbe*, both the 1.5-fold change and 2.0-fold change, at St16 and AFT. In all cases, we noted minimal overlap between the Lbe CNS and muscle target genes (Fig. S19A-D). Not surprisingly, this indicates that the context (CNS versus muscles) greatly influences target gene selection by Lbe.

## DISCUSSION

### Branching terminal selector gene cascade controlling Tv1 neuron identity

The identity of the Tv1 neuron is specified by a genetic cascade that initially commences with a core pathway FFL: *lbe→col→ap/eya* (Baumgardt et al., 2007; Gabilondo et al., 2016). It then forks into three separate branches, with the first branch being a continued FFL of *col→ap/eya→dimm*, which activates Nplp1 neuropeptide expression (Baumgardt et al., 2007; Gabilondo et al., 2016). Recent studies indicate that the entire *lbe→col→ap/eya→dimm→Nplp1* FFL is executed via sequential DNA binding by the TFs onto each enhancer in the cascade (Stratmann and Thor, 2017).

A second branch consists of *dimm* alone, which is necessary and sufficient to activate the regulated secretory pathway, including the neuropeptide-processing machinery and the large dense-core vesicle machinery (Allan et al., 2005; Hamanaka et al., 2010; Hewes et al., 2006; Park et al., 2011). Dimm directly activates *Phm*, and possibly *syta* and *sytb* (Park et al., 2014, 2008a), and acts directly on many other genes in the regulated secretory pathway (Hadžić et al., 2015). Evidence points to Dimm also acting directly on Nplp1 (Stratmann and Thor, 2017), as well as on other neuropeptide genes (Gauthier and Hewes, 2006), and it appears to play a dual role in both activating the regulated secretory pathway and acting combinatorially to activate neuropeptide gene expression (Baumgardt et al., 2007). We find that *col*/*lbe* co-misexpression, which ectopically activates *dimm* in the CNS, results in the activation of most of the previously identified Dimm targets in the regulated secretory pathway.

In contrast to the central role of *dimm* with respect to the regulated secretory pathway, *dimm* does not affect axon pathfinding of Tv1 neurons (Allan et al., 2005). Instead, axon pathfinding is controlled by the third branch, where the *col→ap/eya* and *lbe→col→nerfin-1* FFLs are important for Tv1 axon pathfinding, ensuring that Tv1 axons project towards the midline and join the medial-most FasII-positive fascicle. In line with this model, *nerfin-1* does not affect Nplp1 expression, only pathfinding. The transcriptome and genetic analysis further suggests that the axon pathfinding FFL is itself divided into sub-branches, where *col/lbe* activate the effectors *unc-104*, *gogo* and *futsch*, while *ap/eya* activate (for example) *jeb* and *dnc*. Because *col/lbe* activate *ap/eya*, we cannot rule out a model whereby genes activated by *col/lbe* but not by *ap/eya* still require the combinatorial action of *col/lbe/ap/eya*. However, the lack of ectopic and mutant effects on (for example) *nerfin-1* argues against such a model, at least regarding this downstream target. Thus, the specification of the Tv1 neuron commences with a core initial terminal selector FFL pathway, which branches out into different FLLs, each of which executes different sub-routines that are crucial for final Tv1 identity (Fig. 7). The results from both genome-wide and directed DNA-binding studies (de Taffin et al., 2015; Hadžić et al., 2015; Park et al., 2008a; Stratmann and Thor, 2017) support the hypothesis that these FFLs play out via sequential direct DNA-binding of TFs onto the downstream genes (genes in red in Fig. 7 are predicted to be direct targets for one or several of the upstream TFs).

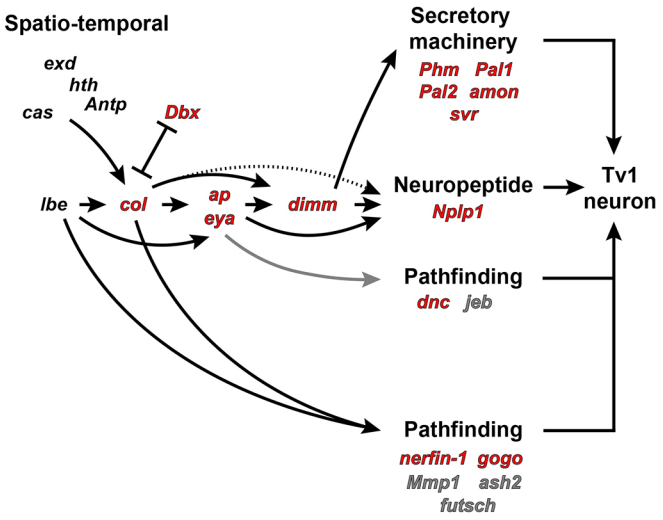


**Fig. 7. Genetic pathways specifying Tv1 neuron cell fate.** The Tv1 cell fate specification cascade. *lbe*, which is selectively expressed by NB5-6 and NB5-3 (De Graeve et al., 2004), acts with the Hox gene *Antp* and the Hox co-factors *hth* and *exd*, as well as the temporal factor *cas*, to trigger expression of *col*. This triggers a feed-forward loop (FFL), modulated by *Dbx*, including the genes *ap, eya* and *dimm*, which act in a combinatorial manner with *lbe* and *col* to specify the terminal cell fate of the Tv1 neuropeptide cells. However, this FFL forks into three different branches, each of which control different subroutines essential for complete Tv1 cell fate. One branch consists of *col→ap/eya→dimm*, which activates Nplp1 neuropeptide expression (Baumgardt et al., 2007; Gabilondo et al., 2016; Stratmann and Thor, 2017). A second branch consists of *dimm* alone, which is necessary and sufficient to activate the regulated secretory pathway, including the neuropeptide-processing machinery and the large dense-core vesicle machinery (Allan et al., 2005; Hadzic et al., 2015; Hamanaka et al., 2010; Hewes et al., 2006; Park et al., 2011, 2014, 2008a,b). The third branch consists of the *col→ap/eya* and *lbe→col→nerfin-1* FFL, which are important for Tv1 axon pathfinding, ensuring that Tv1 axons project towards the midline and join the medial-most FasII-positive fascicle. In line with this model, *nerfin-1* does not affect Nplp1 expression, only pathfinding. Potential downstream factors important for axonal pathfinding are shown in grey, and include *jeb*, *futsch*, *dnc*, *Mmp1* and *ash2*. Thus, the specification of the Tv1 neuron commences with a core initial terminal selector FFL pathway, which branches out into different FLLs, each of which executes different sub-routines crucial for the final Tv1 identity (Fig. 7). Genes in red are putative direct targets of the upstream TFs (see text for details).

Development (2019) 146, dev174300. doi:10.1242/dev.174300

The pleiotropic effects of *Dbx* on Tv1 neuron specification, with both mutants and misexpression affecting several Tv1 properties, including Nplp1 expression, Ap cluster composition and axon pathfinding, makes it difficult at this stage to precisely place *Dbx* within the Tv1 cascade. However, this pleiotropic action is reminiscent of other genes acting in the NB5-6T, such as *Kruppel*, *squeeze*, *nab* and *seven up*, all of which are dynamically expressed during the generation of Ap cluster neurons (Allan et al., 2005; Allan et al., 2003; Baumgardt et al., 2009; Benito-Sipos et al., 2011; Stratmann et al., 2016; Terriente Felix et al., 2007). The surprising apparent lack of Dbx expression in Tv1 neurons or in the NB5-6T lineage may be due to the fact that Dbx is expressed even earlier than was assayed here, or that certain Dbx protein variants are not detected with the antibody used. Alternatively, given the lack of apparent Dbx expression in the NB5-6T lineage, and as the misexpression of *Dbx* was conducted using *elav-Gal4*, a pan-neural driver, it is possible that both the mutant and misexpression phenotypes of *Dbx* reflect non cell-autonomous effects.

One, perhaps unexpected, finding was that although the transcriptome analysis of *col*/*lbe* co-misexpression did reveal twofold upregulation of *ap*, *eya*, *dimm* and *nerfin-1*, it did not reveal upregulation of any additional TFs. The absence of such TFs may suggest that the identified regulators for axon pathfinding (*lbe→co→ap*/*eya*/*nerfin-1*), for Nplp1 (*col→ap*/*eya→dimm*) and for regulated secretory pathway (*dimm*) may indeed constitute the main regulators of these subroutines in Tv1 neurons. This notion is also supported by a recent forward genetic screen, scoring for expression of *FMRFa-eGFP* in the Tv4 Ap cluster neurons, which, although it re-identified *lbe*, *col* and *eya*, did not identify any other late-acting TFs (Bivik et al., 2015). Another unexpected result was that we did not observe twofold upregulation of any obvious axon pathfinding genes, but did identify such genes in the lower (1.5-fold change) group. This could stem from their generally broader expression, which may reduce the fold-change effects in our whole embryo RNA analyses. However, it should also be noted that filtering solely on the GO term 'neuron projection development' may fail to identify some bona fide axon pathfinding genes, and also include genes that are not directly involved in axon pathfinding. Hence, future analysis of the 1075 genes with twofold change and the 3174 genes with 1.5-fold change, affected by *col/lbe* co-misexpression, may help identify additional axon pathfinding genes, as well as further refine the Tv1 neuron genetic cascade.

### One terminal selector versus branching FFLs

The specification of the terminal and unique identity of any given neuron could conceivably be controlled by a number of different mechanisms (Allan and Thor, 2015; Hobert, 2008, 2016; Hobert et al., 2010). Theoretically, one can envision two extreme models: (1) that all aspects of the identity of a neuron could be determined by a single TF; or (2) that all aspects of the fate of a neuron are combinatorially regulated, and that, in addition, there could be considerable branching in the regulatory networks.

Evidence for the first model stems in particular from *C. elegans*, where the TF CHE-1 determines most, if not all, aspects of the identity of a specific gustatory neuron (Etchberger et al., 2007). These studies, and related findings, led the authors to coin the term terminal selectors (Wenick and Hobert, 2004). Similarly, in mammals, the TF Pet-1 acts as a terminal selector, being a key regulator of serotonin neuron specification, controlling genes needed for serotonin synthesis, reuptake and vesicular transport, as well as several other unique features of serotonin neurons (reviewed by Spencer and Deneris, 2017). This scenario, of one factor dictating the entire fate of a neuron, may perhaps have been favoured during evolution, as it may help reduce regulatory complexity.

Support for the second model emerges from the common anatomical scenario where neurons expressing the same neurotransmitter may project axons to different targets. There are many examples of such divergence between transmitter and morphology, e.g. different groups of dopaminergic and serotonergic neurons in the mammalian CNS (Björklund and Dunnett, 2007; Gaspar and Lillesaar, 2012), as well as neuropeptide-producing neurons in many systems (Hokfelt et al., 2000; Park et al., 2008b). Hence, there is an apparent dissociation between neurotransmitter identity and axonal projections, a biological reality that is not easily accommodated by one single TF dictating the entire cell fate. Indeed, studies in *C. elegans* have revealed that the LIM-homeobox gene *ceh-14* only regulates the neuropeptide expression in BDU neurons, but not other aspects of this cell fate (Gordon and Hobert, 2015). Based upon the results reported here, and on previous studies, we find that Tv1 fate is not controlled by one single terminal selector TF, but rather by several combinatorial TFs codes and one single TF (*dimm*), each of which launch different subroutines that are crucial for Tv1 cell fate.

Having the regulatory code for neurotransmitter identity diverge from that controlling axonal pathfinding may better accommodate, even drive, the diverging identities of many neuronal sub-classes during evolution. Furthermore, it would allow for association and disassociation between different terminal neuronal cell fate features. These include association/dissociation of neurotransmitter and cellular morphology, simultaneous or separate production of neuropeptides and small neurotransmitters, coupling-uncoupling of neuropeptide expression with the regulated secretory pathway (scaling). It is tempting to speculate that evolution may have progressed from the basic scenario of one-selector-one-fate to a branching landscape, where every sub-routine of a neuron's property is combinatorially controlled, and where several codes act simultaneously to govern different sub-routines.

## MATERIALS AND METHODS

### Fly stocks

#### Location marker and driver lines

Driver lines used were $wg^{758}$ (referred to as $wg^{Gal4}$; provided by Konrad Basler, University of Zurich, Switzerland), *lbe(K)-Gal4,UAS-EGFP*$^{F}$ [double, i.e. on both chromosome (chr) II and chr III], *lbe(K)-EGFP* (Ulvklo et al., 2012), *apC2.1-tau-lacZ* (chr III) (Lundgren et al., 1995) and $elav^{C155}$=*elav-Gal4* (Bloomington Drosophila Stock Center 458).

#### Mutant lines

Mutant lines used were: $lbe^{12C005}$ (BL#59385); *Df(lbl-lbe)B44* (referred to as $lbe^{Df}$; provided by Krzysztof Jagla, Clermont University, Clermont-Ferrand, France); $col^{1}$ and $col^{3}$ (Crozatier and Vincent, 1999) (provided by Alain Vincent, University Paul Sabatier, Toulouse, France); *Df(2L)BSC354* (referred to as $eya^{Df}$) (BL#24378); $eya^{cli\text{-}IID}$ (BL#3280); $ap^{P44}$ (Bourgouin et al., 1992); $nerfin\text{-}1^{Df}$ (BL#7565); $nerfin\text{-}1^{D159}$ (provided by Alexander Kuzin and Ward Odenwald, NINDS, Bethesda, MD, USA); $Dbx^{D48}$ (BL#56824); $gogo^{H1657}$ and $gogo^{D1600}$ (provided by Takashi Suzuki, Tokyo Institute of Technology, Yokohama, Japan); $futsch^{N94}$ (BL#8805); $unc\text{-}104^{P350}$ (BL#24630) and $unc\text{-}104^{R757}$ (BL#24631).

#### Misexpression lines

Misexpression lines used were: *UAS-col-HA* and *UAS-myc-lbe* (Stratmann et al., 2016); *UAS-Flag-ap* and *UAS-eya-HPC4* (this study); *UAS-nerfin-3xHA* (FlyORF #F000461); and *UAS-Dbx-3xHA* (FlyORF # F001875).

Development (2019) 146, dev174300. doi:10.1242/dev.174300

### CRM line

*Nplp1-CRM-myrRFP-HA* (this study) flies were maintained over *GFP*- or *YFP*-marked balancer chromosomes. Control *OregonR* was used as wild type. Staging of embryos was performed according to Campos-Ortega and Hartenstein (Campos-Ortega and Hartenstein, 1985).

### Immunohistochemistry

Primary antibodies used were: chicken anti-proNplp1 (1:1000), rabbit anti-proFMRFa (1:1000) and guinea pig anti-Dimm (1:1000) (Baumgardt et al., 2007); mouse mAb anti-Eya 10H6 (1:250) and mAb anti-FasII ID4 (1:30) (Developmental Studies Hybridoma Bank); rabbit anti-Ap (1:1000) (Bieli et al., 2015) (provided by Dimi Bieli and Markus Affolter); guinea pig anti-Dbx (1:500) (provided by James B. Skeath, Washington University, St Louis, MO, USA); guinea pig anti-Nerfin-1 (1:500) (provided by Ward Odenwald, NINDS, Bethesda, MD, USA); and goat anti-GFP (1:1000) (ab6673, Abcam).

### *In situ* hybridization

A *nerfin-1* full-length cDNA (LD18634) was obtained from the Drosophila Genomics Resource Center. The authenticity of the cDNA was confirmed by sequencing. The cDNA was linearized using XbaI, and a ribo-probe generated by T7 polymerase. *In situ* hybridization was conducted as previously described (Baumgardt et al., 2007).

### Transgenic flies

#### UAS-constructs

*UAS-Flag-ap* and *UAS-eya-HPC4* were generated by the codon optimization for expression in *Drosophila* (www.kazusa.or.jp/codon/). EcoRI site and consensus start codon (Cavener and Ray, 1991) was added to the 5′ end. Three different stop codons (amb, och, opa) followed by an XbaI site were added to the 3′ end (see Table S1 for DNA sequences). DNAs were generated by gene synthesis (Genscript) and cloned into pUASattB (Bischof et al., 2007) as EcoRI/XbaI fragments. DNAs were injected into landing site strains BL#9723 (28E) for *UAS-Flag-ap* and BL#9744 (89E) for *UAS-eya-HPC4* (BestGene).

#### Nplp1-CRM-myrRFP-HA construction

To generate the Nplp1-CRM-myrRFP-HA.attB landing site construct, first the pEGFP.attB landing site vector (Bischof et al., 2013) (provided by Konrad Basler and Johannes Bischof, University of Zurich, Switzerland) was cut with NdeI and XmaJI in order to remove the GFP cassette. Cutting with NdeI creates a TA overhang compatible with a VspI restriction site, which also creates TA overhangs. A VspI-myrRFP-HA-XmaJI sequence containing the L21 sequence upstream the ATG start codon (Pfeiffer et al., 2012) was synthesized at Genescript and delivered in a pUC57 vector (sequences listed in Table S2). The VspI-myr::RFP-HA-XmaJI construct was cut from the pUC57 vector with VspI and XmaJI, and ligated into the empty attB landing site vector to create a myrRFP-HA.attB vector. The Nplp1 enhancer (Stratmann and Thor, 2017) was generated via PCR on OregonR DNA (primers listed in Table S2) and cloned into the TOPO pCR2.1-TOPO TA vector according to the manufacturer's protocol (Invitrogen). In order to clone the Nplp1-CRM into the myrRFP.attB landing site vector, the myrRFP.attB vector was digested with BglII and XbaI, and the Nplp1-CRM was cut from the TOPO vector with BamHI and XbaI and subsequently ligated upstream the myrRFP-HA cassette. The Nplp1-CRM-myrRFP-HA.attB landing site construct integrated into the fly genome via site directed phiC31 mediated integration (Bischof et al., 2007) at BestGene. Stocks for injection were BL#8622 and BL#9723.

### RNA-sequencing

Per each sample ∼200 embryos of St16 and stage AFT were collected and RNA was isolated from whole embryos (Qiagen RNeasy Mini kit, 74104). For each genotype and stage, three independent biological replicates were prepared. RNA-sequencing library preparation was carried out using the NEBNext Ultra RNA Library Prep Kit for Illumina by following manufacturer's recommendations (NEB). The samples were sequenced on the Illumina Hiseq 2500 platform using a 1×50 bp configuration for all stage AFT samples and a 2×150 bp paired end configuration for all St16 samples, with a depth of ∼30-50 million reads. (GeneWiz). FASTQ files were pseudoaligned to the *Drosophila melanogaster* coding sequences (CDS, BDGP6, ensemble.org), abundances of transcripts were determined using Kallisto (release 0.43.1) as transcripts per million (TPM) units (Bray et al., 2016). Genes of interest were identified based on TPMs being different by at least 2FCs and overlapping with the GO-term gene list GO0031175 neuron-projection-development for *Dmel* (amigo.geneontology.org/amigo/term/GO:0031175). Genes are presented in heatmaps and Venn diagrams. The RNA-seq files have been deposited in GEO under accession number GSE113260.

### Confocal imaging and data acquisition

Zeiss LSM700 or LSM800 confocal microscopes were used for fluorescent images; confocal stacks were merged using LSM software or ImageJ FIJI. Statistic calculations were performed in Graphpad prism software (v4.03). Cell counts and reporter (GFP) measurements were carried out using ImageJ FIJI and numbers were transferred to Graphpad prism. To address statistical significance, Student's *t*-test was used. Images and graphs were compiled in Adobe Illustrator. The numerical data underlying the graphs in the figures are included in Table S3.

#### Acknowledgements

We are grateful to Ward Odenwald, Alexander Kuzin, James B. Skeath, Alain Vincent, Krzysztof Jagla, Dimi Bieli, Markus Affolter, Takashi Suzuki, Konrad Basler, Johannes Bischof, the Drosophila Genomics Resource Center, the Developmental Studies Hybridoma Bank at the University of Iowa, the Bloomington Stock Center and the FlyORF stock center for sharing antibodies, fly lines and DNAs. We thank Doug W. Allan, John B. Thomas and Chris Q. Doe for critically reading the manuscript. We thank Erik Hultin for his help on this project during the course of his Bachelor thesis project. Behzad Salmani Yaghmaeian, Carolin Jonsson and Annika Starkenberg provided excellent technical assistance.

#### Competing interests

The authors declare no competing or financial interests.

#### Author contributions

Conceptualization: S.T., J.S.; Methodology: J.S., H.E.; Formal analysis: J.S., H.E.; Investigation: J.S., H.E.; Resources: S.T.; Data curation: J.S.; Writing - original draft: S.T., J.S.; Writing - review & editing: S.T., J.S.; Visualization: J.S.; Supervision: S.T.; Project administration: S.T.; Funding acquisition: S.T.

#### Funding

Funding was provided by the Vetenskapsrådet (621-2013-5258, 2017-0440601), the Knut och Alice Wallenbergs Stiftelse (KAW2011.0165, KAW2012.0101, KAW2017.0312) and the Cancerfonden (140780, 150663, CAN2017/257) to S.T.

#### Data availability

The RNA-seq files have been deposited in GEO under accession number GSE113260.

#### Supplementary information

Supplementary information available online at
http://dev.biologists.org/lookup/doi/10.1242/dev.174300.supplemental

#### References

**Allan, D. W. and Thor, S.** (2015). Transcriptional selectors, masters, and combinatorial codes: regulatory principles of neural subtype specification. *Wiley Interdiscip. Rev. Dev. Biol.* **4**, 505-528.

**Allan, D. W., Pierre, S. E. S., Miguel-Aliaga, I. and Thor, S.** (2003). Specification of neuropeptide cell identity by the integration of retrograde BMP signaling and a combinatorial transcription factor code. *Cell* **113**, 73-86.

**Allan, D. W., Park, D., St Pierre, S. E., Taghert, P. H. and Thor, S.** (2005). Regulators acting in combinatorial codes also act independently in single differentiating neurons. *Neuron* **45**, 689-700.

**Barkus, R. V., Klyachko, O., Horiuchi, D., Dickson, B. J. and Saxton, W. M.** (2008). Identification of an axonal kinesin-3 motor for fast anterograde vesicle transport that facilitates retrograde transport of neuropeptides. *Mol. Biol. Cell* **19**, 274-283.

**Baumgardt, M., Miguel-Aliaga, I., Karlsson, D., Ekman, H. and Thor, S.** (2007). Specification of neuronal identities by feedforward combinatorial coding. *PLoS Biol.* **5**, 295-308.

**Baumgardt, M., Karlsson, D., Terriente, J., Díaz-Benjumea, F. J. and Thor, S.** (2009). Neuronal subtype specification within a lineage by opposing temporal feed-forward loops. *Cell* **139**, 969-982.

**Benito-Sipos, J., Ulvklo, C., Gabilondo, H., Baumgardt, M., Angel, A., Torroja, L. and Thor, S.** (2011). Seven up acts as a temporal factor during two different stages of neuroblast 5-6 development. *Development* **138**, 5311-5320.
**Berger, J., Senti, K.-A., Senti, G., Newsome, T. P., Åsling, B., Dickson, B. J. and Suzuki, T.** (2008). Systematic identification of genes that regulate neuronal wiring in the Drosophila visual system. *PLoS Genet.* **4**, e1000085.
**Bieli, D., Kanca, O., Gohl, D., Denes, A., Schedl, P., Affolter, M. and Muller, M.** (2015). The Drosophila melanogaster mutants apblot and apXasta affect an essential apterous wing Enhancer. *G3 (Bethesda)* **5**, 1129-1143.
**Bischof, J., Maeda, R. K., Hediger, M., Karch, F. and Basler, K.** (2007). An optimized transgenesis system for Drosophila using germ-line-specific phiC31 integrases. *Proc. Natl. Acad. Sci. USA* **104**, 3312-3317.
**Bischof, J., Bjorklund, M., Furger, E., Schertel, C., Taipale, J. and Basler, K.** (2013). A versatile platform for creating a comprehensive UAS-ORFeome library in Drosophila. *Development* **140**, 2434-2442.
**Bivik, C., Bahrampour, S., Ulvklo, C., Nilsson, P., Angel, A., Fransson, F., Lundin, E., Renhorn, J. and Thor, S.** (2015). Novel genes involved in controlling specification of Drosophila FMRFamide neuropeptide cells. *Genetics* **200**, 1229-1244.
**Björklund, A. and Dunnett, S. B.** (2007). Dopamine neuron systems in the brain: an update. *Trends Neurosci.* **30**, 194-202.
**Bourgouin, C., Lundgren, S. E. and Thomas, J. B.** (1992). *Apterous* is a *Drosophila* LIM domain gene required for the development of a subset of embryonic muscles. *Neuron* **9**, 549-561.
**Bray, N. L., Pimentel, H., Melsted, P. and Pachter, L.** (2016). Near-optimal probabilistic RNA-seq quantification. *Nat. Biotechnol.* **34**, 525-527.
**Campos-Ortega, J. A. and Hartenstein, V.** (1985). *The Embryonic Development of Drosophila Melanogaster*. New York: Springer-Verlag.
**Cavener, D. R. and Ray, S. C.** (1991). Eukaryotic start and stop translation sites. *Nucleic Acids Res.* **19**, 3185-3192.
**Chu-LaGraff, Q. and Doe, C. Q.** (1993). Neuroblast specification and formation regulated by wingless in the Drosophila CNS. *Science* **261**, 1594-1597.
**Crozatier, M. and Vincent, A.** (1999). Requirement for the Drosophila COE transcription factor Collier in formation of an embryonic muscle: transcriptional response to notch signalling. *Development* **126**, 1495-1504.
**De Graeve, F., Jagla, T., Daponte, J.-P., Rickert, C., Dastugue, B., Urban, J. and Jagla, K.** (2004). The ladybird homeobox genes are essential for the specification of a subpopulation of neural cells. *Dev. Biol.* **270**, 122-134.
**de Taffin, M., Carrier, Y., Dubois, L., Bataille, L., Painset, A., Le Gras, S., Jost, B., Crozatier, M. and Vincent, A.** (2015). Genome-wide mapping of collier in vivo binding sites highlights its hierarchical position in different transcription regulatory networks. *PLoS ONE* **10**, e0133387.
**Etchberger, J. F., Lorch, A., Sleumer, M. C., Zapf, R., Jones, S. J., Marra, M. A., Holt, R. A., Moerman, D. G. and Hobert, O.** (2007). The molecular signature and cis-regulatory architecture of a C. elegans gustatory neuron. *Genes Dev.* **21**, 1653-1674.
**Gabilondo, H., Stratmann, J., Rubio-Ferrera, I., Millán-Crespo, I., Contero-García, P., Bahrampour, S., Thor, S. and Benito-Sipos, J.** (2016). Neuronal cell fate specification by the convergence of different spatiotemporal cues on a common terminal selector cascade. *PLoS Biol.* **14**, e1002450.
**Gaspar, P. and Lillesaar, C.** (2012). Probing the diversity of serotonin neurons. *Philos. Trans. R. Soc. Lond. B Biol. Sci.* **367**, 2382-2394.
**Gauthier, S. A. and Hewes, R. S.** (2006). Transcriptional regulation of neuropeptide and peptide hormone expression by the Drosophila dimmed and cryptocephal genes. *J. Exp. Biol.* **209**, 1803-1815.
**Gordon, P. M. and Hobert, O.** (2015). A competition mechanism for a homeotic neuron identity transformation in C. elegans. *Dev. Cell* **34**, 206-219.
**Hadžić, T., Park, D., Abruzzi, K. C., Yang, L., Trigg, J. S., Rohs, R., Rosbash, M. and Taghert, P. H.** (2015). Genome-wide features of neuroendocrine regulation in Drosophila by the basic helix-loop-helix transcription factor DIMMED. *Nucleic Acids Res.* **43**, 2199-2215.
**Hamanaka, Y., Park, D., Yin, P., Annangudi, S. P., Edwards, T. N., Sweedler, J., Meinertzhagen, I. A. and Taghert, P. H.** (2010). Transcriptional orchestration of the regulated secretory pathway in neurons by the bHLH protein DIMM. *Curr. Biol.* **20**, 9-18.
**Hewes, R. S., Gu, T., Brewster, J. A., Qu, C. and Zhao, T.** (2006). Regulation of secretory protein expression in mature cells by DIMM, a basic helix-loop-helix neuroendocrine differentiation factor. *J. Neurosci.* **26**, 7860-7869.
**Hobert, O.** (2008). Regulatory logic of neuronal diversity: terminal selector genes and selector motifs. *Proc. Natl. Acad. Sci. USA* **105**, 20067-20071.
**Hobert, O.** (2016). Terminal selectors of neuronal identity. *Curr. Top. Dev. Biol.* **116**, 455-475.
**Hobert, O., Carrera, I. and Stefanakis, N.** (2010). The molecular and gene regulatory signature of a neuron. *Trends Neurosci.* **33**, 435-445.
**Hokfelt, T., Broberger, C., Xu, Z.-Q. D., Sergeyev, V., Ubink, R. and Diez, M.** (2000). Neuropeptides–an overview. *Neuropharmacology* **39**, 1337-1356.
**Hummel, T., Krukkert, K., Roos, J., Davis, G. and Klambt, C.** (2000). *Drosophila* Futsch/22C10 is a MAP1B-like protein required for dendritic and axonal development. *Neuron* **26**, 357-370.
**Junion, G., Bataille, L., Jagla, T., Da Ponte, J. P., Tapin, R. and Jagla, K.** (2007). Genome-wide view of cell fate specification: ladybird acts at multiple levels during diversification of muscle and heart precursors. *Genes Dev.* **21**, 3163-3180.
**Karlsson, D., Baumgardt, M. and Thor, S.** (2010). Segment-specific neuronal subtype specification by the integration of anteroposterior and temporal cues. *PLoS Biol.* **8**, e1000368.
**Kuzin, A., Brody, T., Moore, A. W. and Odenwald, W. F.** (2005). Nerfin-1 is required for early axon guidance decisions in the developing Drosophila CNS. *Dev. Biol.* **277**, 347-365.
**Lacin, H., Zhu, Y., Wilson, B. A. and Skeath, J. B.** (2009). dbx mediates neuronal specification and differentiation through cross-repressive, lineage-specific interactions with eve and hb9. *Development* **136**, 3257-3266.
**Lim, A., Rechtsteiner, A. and Saxton, W. M.** (2017). Two kinesins drive anterograde neuropeptide transport. *Mol. Biol. Cell* **28**, 3542-3553.
**Lundgren, S. E., Callahan, C. A., Thor, S. and Thomas, J. B.** (1995). Control of neuronal pathway selection by the *Drosophila* LIM homeodomain gene *apterous*. *Development* **121**, 1769-1773.
**Medina, P. M. B., Swick, L. L., Andersen, R., Blalock, Z. and Brenman, J. E.** (2006). A novel forward genetic screen for identifying mutations affecting larval neuronal dendrite development in Drosophila melanogaster. *Genetics* **172**, 2325-2335.
**Miguel-Aliaga, I., Allan, D. W. and Thor, S.** (2004). Independent roles of the dachshund and eyes absent genes in BMP signaling, axon pathfinding and neuronal specification. *Development* **131**, 5837-5848.
**Park, D. and Taghert, P. H.** (2009). Peptidergic neurosecretory cells in insects: organization and control by the bHLH protein DIMMED. *Gen. Comp. Endocrinol.* **162**, 2-7.
**Park, D., Han, M., Kim, Y.-C., Han, K.-A. and Taghert, P. H.** (2004). Ap-let neurons–a peptidergic circuit potentially controlling ecdysial behavior in Drosophila. *Dev. Biol.* **269**, 95-108.
**Park, D., Shafer, O. T., Shepherd, S. P., Suh, H., Trigg, J. S. and Taghert, P. H.** (2008a). The Drosophila basic helix-loop-helix protein DIMMED directly activates PHM, a gene encoding a neuropeptide-amidating enzyme. *Mol. Cell. Biol.* **28**, 410-421.
**Park, D., Veenstra, J. A., Park, J. H. and Taghert, P. H.** (2008b). Mapping peptidergic cells in Drosophila: where DIMM fits in. *PLoS ONE* **3**, e1896.
**Park, D., Hadžić, T., Yin, P., Rusch, J., Abruzzi, K., Rosbash, M., Skeath, J. B., Panda, S., Sweedler, J. V. and Taghert, P. H.** (2011). Molecular organization of Drosophila neuroendocrine cells by Dimmed. *Curr. Biol.* **21**, 1515-1524.
**Park, D., Li, P., Dani, A. and Taghert, P. H.** (2014). Peptidergic cell-specific synaptotagmins in Drosophila: localization to dense-core granules and regulation by the bHLH protein DIMMED. *J. Neurosci.* **34**, 13195-13207.
**Pfeiffer, B. D., Truman, J. W. and Rubin, G. M.** (2012). Using translational enhancers to increase transgene expression in Drosophila. *Proc. Natl. Acad. Sci. USA* **109**, 6626-6631.
**Roos, J., Hummel, T., Ng, N., Klämbt, C. and Davis, G. W.** (2000). Drosophila Futsch regulates synaptic microtubule organization and is necessary for synaptic growth. *Neuron* **26**, 371-382.
**Schmid, A., Chiba, A. and Doe, C. Q.** (1999). Clonal analysis of Drosophila embryonic neuroblasts: neural cell types, axon projections and muscle targets. *Development* **126**, 4653-4689.
**Schmidt, H., Rickert, C., Bossing, T., Vef, O., Urban, J. and Technau, G. M.** (1997). The embryonic central nervous system lineages of Drosophila melanogaster. II. Neuroblast lineages derived from the dorsal part of the neuroectoderm. *Dev. Biol.* **189**, 186-204.
**Spencer, W. C. and Deneris, E. S.** (2017). Regulatory Mechanisms Controlling Maturation of Serotonin Neuron Identity and Function. *Front. Cell. Neurosci.* **11**, 215.
**Stivers, C., Brody, T., Kuzin, A. and Odenwald, W. F.** (2000). Nerfin-1 and –2, novel Drosophila Zn-finger transcription factor genes expressed in the developing nervous system. *Mech. Dev.* **97**, 205-210.
**Stratmann, J. and Thor, S.** (2017). Neuronal cell fate specification by the molecular convergence of different spatio-temporal cues on a common initiator terminal selector gene. *PLoS Genet.* **13**, e1006729.
**Stratmann, J., Gabilondo, H., Benito-Sipos, J. and Thor, S.** (2016). Neuronal cell fate diversification controlled by sub-temporal action of Kruppel. *eLife* **5**, e19311.
**Terriente Felix, J., Magarinos, M. and Diaz-Benjumea, F. J.** (2007). Nab controls the activity of the zinc-finger transcription factors Squeeze and Rotund in Drosophila development. *Development* **134**, 1845-1852.
**Tomasi, T., Hakeda-Suzuki, S., Ohler, S., Schleiffer, A. and Suzuki, T.** (2008). The transmembrane protein Golden goal regulates R8 photoreceptor axon-axon and axon-target interactions. *Neuron* **57**, 691-704.
**Ulvklo, C., Macdonald, R., Bivik, C., Baumgardt, M., Karlsson, D. and Thor, S.** (2012). Control of neuronal cell fate and number by integration of distinct daughter cell proliferation modes with temporal progression. *Development* **139**, 678-689.
**Wenick, A. S. and Hobert, O.** (2004). Genomic cis-regulatory architecture and trans-acting regulators of a single interneuron-specific gene battery in C. elegans. *Dev. Cell* **6**, 757-770.